



HYPERSPECTRAL REMOTE SENSING FOR ADVANCED DETECTION OF EARLY BLIGHT (ALTERNARIA SOLANI) DISEASE IN POTATO (SOLANUM TUBEROSUM) PLANTS PRIOR TO VISUAL DISEASE SYMPTOMS

Daniel Atherton¹, Ruplal Choudhary², and Dennis Watson²


¹School of Agriculture, College of Business & Technology, Western Illinois University, Macomb, IL 61455

²Department of Plant, Soil and Agricultural Systems, College of Agricultural Sciences, Southern Illinois University, Carbondale, IL 62901

ABSTRACT: Early detection of disease and insect infestation within crops is essential to reduce potential production losses, reduce environmental risk, and reduce the cost of farming. The objective of this study was the detection of early blight (*Alternaria solani*) in potato (*Solanum tuberosum*) plants at two different growth stages using a handheld hyperspectral spectroradiometer. Hyperspectral reflectance spectra were captured 10 times over five weeks from plants grown to the vegetative and tuber bulking growth stages. The spectra were analyzed using cluster analysis and the vegetative indices, simple ratio (SR) and normalized difference vegetative index (NDVI). For SR, wavelengths used were 665 nm and 770 nm; for NDVI, wavelengths used were 670, 695, 735, and 945 nm. Both cluster analysis and the vegetative indices SR and NDVI successfully distinguished moderately diseased plants from healthy and minimally diseased plants. This study demonstrated the capability of cluster analysis and the vegetative indices SR and NDVI for the detection of early blight in potato plants.

Key words: Early Blight, Potato, Remote Sensing, Spectroradiometer.

*Corresponding author: Daniel Atherton, School of Agriculture, College of Business & Technology, Western Illinois University, Macomb, IL 61455 E-mail : dl-atherton@wiu.edu

Copyright: ©2017 Daniel Atherton. This is an open-access article distributed under the terms of the Creative Commons Attribution License , which permits unrestricted use, distribution, and reproduction in any medium, provided the original author and source are credited

INTRODUCTION

Remote sensing continues to be a promising field with the ability to distinguish slight variations in the reflectance of crop foliage providing data for more precise production of crops throughout the growing season. Vegetation reflects a varying amount of energy in the visible and infrared wavelength spectrums depending on vegetation type and health of the vegetation. When plants suffer from a stress factor such as nutrient deficiency, drought, pest or disease infestation, normal chlorophyll production diminishes followed by a decrease in absorption in the red and blue regions and an increase in reflectance in these regions [39]. The relation between cause and effect allows establishment of empirical relationships between factors causing plant stress and the resulting reflectance signatures [18]. Traditional methods of pigment analysis (chlorophylls, carotenoids, and anthocyanins) to determine crop status are time consuming, expensive, and require destruction of measured leaves; whereas spectral reflectance measurements provide a means to determine pigment content with a rapid, non-invasive technique [11]. Many researchers have analyzed pigment levels in vegetation with reflectance data at specific wavelengths or by creating ratios of reflectance data values at several specific wavelengths [5], [6], [10], [11], [15], and [32] or at the red-edge [21].

Remote sensing data provides a means for early detection of disease and insect infestation within crops to help reduce potential production losses, lessen environmental risk, and decrease the cost of farming. [43] reported large-scale tomato growers apply pesticides, especially fungicides, on a calendar-based application schedule because the treatment window can be very short for their high-value crops. The fungus late blight, *Phytophthora infestans*, which has a treatment window of one week, is an example of a fungus with a short treatment window. According to [25], *P. infestans* slashes global potato production by approximately 15%, but one in every three to four years in India, the losses are much greater. Depending upon weather conditions and the specific area, late blight can slash yield up to 75% in major potato producing regions of India making early detection essential for disease control [25]. Another example of the high cost of agricultural pests is the Russian wheat aphid, *Diuraphis noxia*, which was first identified in the United States in 1986 and now causes an estimated loss to the U.S. small grain industry of over one billion dollars annually [4]. According to [4], ground field surveying revealed that stress in wheat fields is not uniformly distributed; some areas are highly stressed and other areas are completely stress-free. One may consider aggressive crop scouting to be the solution to aggressive diseases, but according to [44], conventional ground scouting has not provided an efficient means of detection and monitoring for large tomato crops. To prevent overuse of chemicals, growers need a remote sensing system that can provide timely detection of diseases [43].

Regardless of whether high value crops are infected with a disease, growers typically apply pesticides as insurance to minimize the risk of losing large amounts of their crop. Agricultural growers spray chemicals uniformly over entire fields to control disease, which is needlessly expensive since disease infestation is predominately concentrated in patches around original foci where disease originates [22], with large areas of fields free from disease at any stage of infestation [7]. In addition to incurring a higher production cost, continual application of pesticides increases the risk of pests adapting to pesticides, rendering the pesticides ineffective. Uniform spraying may increase the level of toxic residues and contamination of ground water, which makes targeted pesticide placement at the correct time an important goal.

Advanced detection of diseases like late blight and early blight is needed so the correct pesticide can be applied at the proper rate at the best time and optimum location to minimize input costs and reduce possible damage from over-application of pesticides to the crop and to the environment. Growers need advanced remote sensing research and tools to provide early detection of diseases and pests for accurate treatment.

RESEARCH OBJECTIVE

The objective of this study was the differentiation of early blight (*Alternaria solani*) diseased potato (*Solanum tuberosum*) plants from healthy potato plants at two growth stages using a hyperspectral spectroradiometer prior to definitive identification of early blight disease using visual disease symptomology.

MATERIALS AND METHODS

Experimental Design

The two experiments consisted of potato variety *Solanum tuberosum* cv. 'Yukon Gold' grown to the vegetative (3-6 weeks) and tuber bulking (8-12 weeks) growth stages [23]. The Yukon Gold cultivar was developed at the University of Guelph (Ontario, Canada) in 1966 and registered in Canada in 1980 [8]. Each experiment consisted of the single factor, disease rating (Table 1), with repeated measures of two reflectance data capture events "measurement events" per week for 5 weeks for a total of 10 spectral data capture events. The 5-week period extended from time of disease inoculation until a majority of inoculated plants suffered from multiple early blight blotches ("bull's eyes") on over half of the plant's leaves. A disease rating system was adapted from [42] and detailed in Table 1 and Figure 1. Immediately prior to each measurement event, each plant was examined and assigned a disease rating. The reflectance values captured during each measurement event served as the independent variable.

Table 1. Disease Progression Rating Levels

Rating Level	Description
R0	Healthy plant - no indication of disease
R1	Small spots on one or two leaves of plant canopy, no "bulls eyes"
R2	Small spots on more than two leaves & less than half of plant canopy, no "bulls eyes"
R3	Small spots on more than half of plant canopy, no "bull's eyes"
R4	Single "bull's eye" (with spots) on one or two leaves of plant canopy
R5	Multiple "bull's eyes" (with spots) on more than two leaves, but less than half of plant canopy
R6	Multiple "bull's eyes" (with spots) on more than half of plant canopy

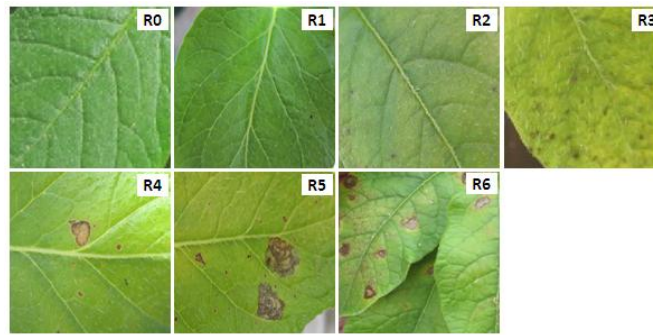


Figure 1. Disease progression by rating level

HYPERSPECTRAL REFLECTANCE EQUIPMENT

The instrumentation used to capture hyperspectral reflectance signatures from the potato plants in this study was an ASD FieldSpec® 3 spectroradiometer (ASD Inc., Boulder, CO) with a spectral range of 350–1,800 nm and a spectral resolution of 3 nm Full-Width-Half-Maximum (FWHM) at 700 nm and 10 nm FWHM at 1,400 nm. The spectroradiometer's sampling interval for the 350–1,000 nm range was 1.4 nm and 2 nm in the 1,000–1,800 nm range. A white reference panel that reflects nearly 100% of ambient energy was used for light source calibration.

POTATO PLANTS AND INOCULATION

A greenhouse at the Horticulture Research Center of Southern Illinois University (Carbondale, Illinois) was used to house two nearly identical controlled environment chambers to isolate potato plants used in the study from the introduction of pathogens or other outside factors. Potatoes were planted in one gallon plastic nursery pots filled 90% full with Fafard® Growing Mix 2 (Sun Gro®, Pine Bluff, AR) plant bedding material on May 10th and June 21st, 42 days apart so at the time of inoculation with the *Alternaria solani* pathogen, one set of plants were within the vegetative growth stage while the other set of plants were within the tuber bulking growth stage. The two separate plantings ensured plants within the two growth stages could be differentiated as healthy or infected. Each planting consisted of four replicates [37] and [40] of control and infected plants for a total of eight Yukon Gold potato plants per growth stage. All plants were watered daily. Osmocote Smart-Release® 14-14-14 (NPK) granular plant food (15 grams) was applied to each pot after planting and approximately 8 weeks thereafter. On a weekly basis, prior to inoculation with *A. solani*, each plant was randomly moved to either a new location within the same chamber or to the other chamber to minimize microclimate effects.

At time of inoculation, an equal quantity of vegetative and tuber bulking plants were randomly segregated into either the first or second chamber. The first chamber became the control chamber and the second chamber became the inoculation chamber. *A. solani* conidia inoculum with a concentration of 5×10^6 conidia per mL was applied to the foliage of each plant in the inoculation chamber at a rate of roughly 4 mL per plant using a spray bottle. Koch's [31] postulates were fulfilled while generating *A. solani* conidia for this study. A humidifier (Hydrofogger®, Hydrofogger.com, Greenville, SC) was incorporated into the inoculation chamber to provide sufficient humidity to aid in germination of the *A. solani* pathogen. Humidity was maintained at about 95% for the first 48 hours after inoculation. Each day thereafter, the humidifier was operated to increase relative humidity to 90 - 95% for 6 to 8 hours during the hottest time of the day to minimize heat buildup and encourage additional spore germination, which can occur within several hours once moisture is present on foliage, then humidity was allowed to drop to the ambient humidity level for the remainder of the day.

HYPERSPECTRAL DATA COLLECTION

Hyperspectral reflectance signatures were captured from each plant on the day of inoculation, (just prior to inoculation) and four days thereafter and was repeated weekly for a total of 5 weeks or 10 measurement events. Measurement protocols were established to minimize environmental variability. Reflectance data was captured prior to daily plant watering for plant moisture consistency. Signatures were captured between 11:00 am and 1:00 pm to maximize sunlight. The spectroradiometer was allowed to operate for at least 20 minutes prior to capturing reflectance data to avoid steps between wavelength regions due to different warmup rates for each sensor within the spectrometer. Each plant was centered (nadir) under the radiometer's fiber optic input, which was mounted at a distance sufficient to achieve an instantaneous field of view consisting of roughly 80% of the plant's canopy. The spectrometer was calibrated using the white reference panel prior to capturing reflectance data from each plant. Then the radiometer was engaged to capture 10 hyperspectral curves from the plant over a period of about 15 seconds to minimize variance from the calibrated state.

Reflectance curves were first captured from control plants, followed by inoculated plants to reduce the risk of contaminating control plants from prior handling of inoculated plants. The ordering of plants within the control group and within the inoculated group was random. Plants were returned to each chamber in a different location to reduce microclimate effects. Mapping between each plant's identification tag and the captured reflectance files for each plant was logged to ensure each reflectance file could be linked to the plant responsible for the reflectance curve. The hyperspectral curve data was then stored for subsequent data analysis.

HYPERSPECTRAL DATA PRE-PROCESSING

The 10 raw hyperspectral data curves captured for each plant during each measurement event were modified to remove wavelengths between 1355-1415 nm due to high levels of noise caused by atmosphere water vapor [2] and between 350-400 nm due to high levels of noise [1]. The hyperspectral data curves were then pre-processed similar to [42] to retain reflectance values within two standard deviations of the mean of the reflectance values at each wavelength for each plant of each measurement event. Each reflectance value was compared to the mean of the other nine values at the same wavelength to determine if each value was within two standard deviations of the mean. Most of the 13,420 original reflectance values per measurement event were retained with only 0.86% of the reflectance values dropped. At each wavelength, the mean of the retained reflectance values was calculated for each plant of each measurement event, like [25], to obtain an initial composite signature.

Prior studies like [35] demonstrated bands in close proximity provide redundant information. Some researchers [19] made effective use of composite signatures averaged over 10 nm intervals. To achieve a balance between averaging at 10 nm intervals and ensuring information was not lost, composite signatures were averaged at five nm intervals which resulted in 270 wavelengths. First order derivative signatures with five nm interval were generated from initial composite signatures.

HYPERSPECTRAL DATA ANALYSIS

Cluster Analysis

Analysis of the reflectance data was conducted using two complementary methods. The first method used was cluster analysis, which is an unsupervised classification method that finds clusters of natural groupings in the dataset, requiring no training dataset. [42] demonstrated the ability to distinguish healthy tomato plants from late blight infected plants using cluster analysis in several fields of tomatoes with varying levels of infection. More heavily diseased plants that reached the point of economic loss could be discriminated from healthy and minimally diseased plants [42]. As noted by [42], two concerns need to be addressed when using clustering analysis. The first concern is determining the number of groups in which to cluster the dataset and the second concern is deciding whether a solution, once found, is actually significant. Most methods used for clustering analysis are biased towards producing clusters with a certain shape, size, or dispersion, so one must review the results and decide whether the generated clusters represent the groupings expected for the specific dataset [29]. PROC CLUSTER [30] was configured to use the centroid method based on squared Euclidean distance, since it minimizes size and dispersion biases inherent in other methods [29].

Vegetative Indices

The second method used for analysis was vegetative indices. It was suggested by [20] that a vegetative index should maximize sensitivity to plant biophysical properties, normalize effects due to angle of radiance and viewing angle, normalize effects such as variations in canopy structure or in soils, and be linked to biophysical properties to validate the vegetative index. Many researchers have used indices to analyze spectra for moisture monitoring [26], [27], and [41]; yield estimation [38]; nutrient monitoring [9], [16], [34], [37], and [45]; insect [24] and disease detection [17], [25], [33], and [43].

One issue with vegetative indices is the difficulty of developing an index sensitive to only the target factor and insensitive to all other factors [14]. The number of vegetative indices continues to grow [17], [25], [26], [33], [38], [43], and [45]; as researchers make improvements to existing indices or develop new indices to derive information from reflectance data. Indices are gaining in complexity [9], [24], and [41] with use of higher spatial and spectral resolution imagery.

SR and NDVI were used due to their ability to detect differences in vegetation caused by stress factors with most new indices [9], [24], and [41], being variations of the original SR and NDVI. A comprehensive analysis of each wavelength combination was made using the simple ratio (1):

$$SR = \lambda_{NIR} / \lambda_R \quad (1)$$

and the normalized difference vegetative index (2):

$$NDVI = (\lambda_{NIR} - \lambda_R) / (\lambda_{NIR} + \lambda_R) \quad (2)$$

where λ is the reflectance value at the designated wavelength, NIR is the near-infrared wavelength region (~700 -1,000 nm), and R is the visible red wavelength region (~610-690 nm), to determine which wavelengths were most sensitive (greatest ratio difference) when comparing diseased plant reflectance to healthy plant reflectance.

These wavelengths were used to generate indices for healthy and diseased plants as the disease progressed during the experiment. To determine the statistical significance between the indices at various stages of disease progression, the indices were analyzed using an Analysis of Variance (ANOVA) and t-test with PROC GLM and PROC TTEST [28]. An alpha level of 0.05 was used as the level of significance for the analyses.

RESULTS

Cluster Analysis

Clustering was completed on each experiment for the 10 measurement events, similar to [42]. The clustering operation produced tree diagrams (dendrograms) that were analyzed to determine the optimal number of clusters for differentiation between healthy and diseased plants. For brevity, four tree diagrams for the VG and TB stages are displayed in Figures 2 and 3, respectively. The clusters within each tree diagram were summarized using the plants' ratings to provide a percentage distribution of the composite membership of each cluster at each of the three centroid distance thresholds of 0.5, 0.75, and 1.0. The summarized data for the tree diagrams in Figures 2 and 3 can be found listed in Tables 2 and 3, respectively.

For brevity, only results presented in Table 2 (YG in VG stage) are reviewed here. Starting on 8/18 and progressing in reverse chronological order over the four measurement events, one can review the cluster membership to determine the optimal threshold for the clustering algorithm and observe the efficacy of distinction between healthy and diseased plants. Clustering for the VG stage on 8/18 required 4, 3, and 2 clusters for the 0.5, 0.75, and 1.0 thresholds, respectively. Cluster membership was R5 (50%) and R6 (50%) for cluster 1 and R0 for clusters 2, 3, and 4 for the 0.5 threshold; R5 (50%) and R6 (50%) for cluster 1 and R0 for clusters 2 and 3 for the 0.75 threshold; and R0 (33%), R5 (33%), and R6 (33%) for cluster 1 and R0 for cluster 2 for the 1.0 threshold. Clustering for 8/11 required 2 clusters for all thresholds. Cluster membership was R4 (75%) and R5 (25%) for cluster 1 and R0 for cluster 2 for all thresholds. Clustering for 8/4 required 4, 3, and 2 clusters for the 0.5, 0.75, and 1.0 thresholds, respectively. Cluster membership was R2 for clusters 1 and 2, R2 (50%) and R4 (50%) for cluster 3, and R0 for cluster 4 for the 0.5 threshold; R2 for cluster 1, R2 (67%) and R4 (33%) for cluster 2, and R0 for cluster 3 for the 0.75 threshold; and R2 for cluster 1, R0 (57%), R2 (29%), and R4 (14%) for cluster 2 for the 1.0 threshold. Clustering for 7/28 required 3, 2, and 2 clusters for the 0.5, 0.75, 1.0 thresholds. Cluster membership was R1 (50%) and R2 (50%) for cluster 1, R0 (75%) and R1 (25%) for cluster 2, R0 (50%) and R1 (50%) for cluster 3 for 0.5 threshold; R1 (50%) and R2 (50%) for cluster 1, R0 (67%) and R1 (33%) for cluster 2 for 0.75 and 1.0 thresholds.

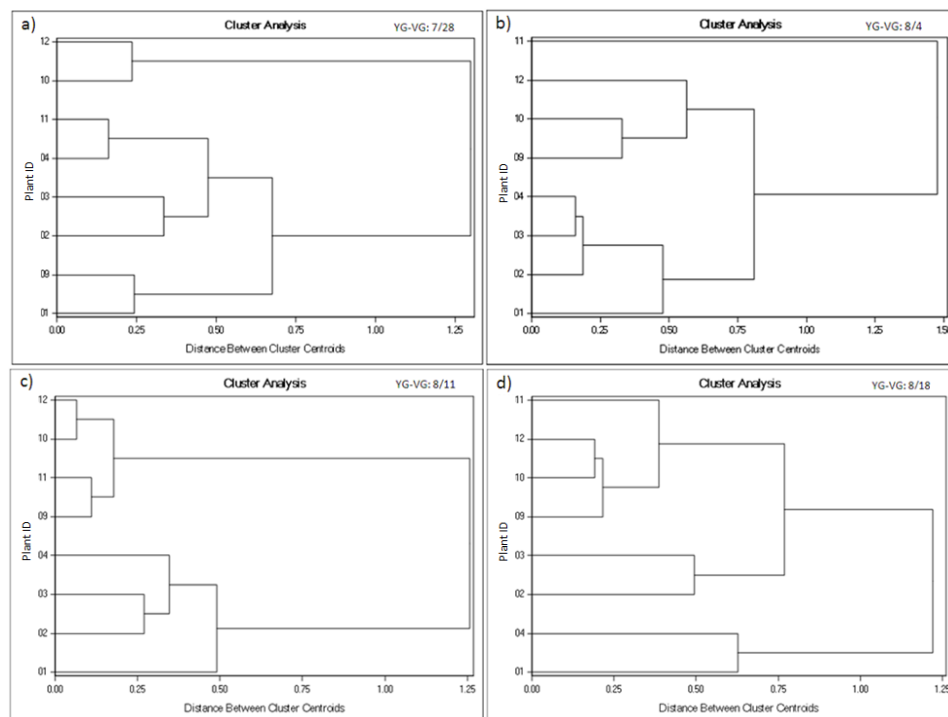


Figure 2. Tree diagrams for vegetative (VG) stage on: a) 7/28; b) 8/4; c) 8/11; d) 8/18. Plants 01, 02, 03, and 04 are control plants; plants 09, 10, 11, and 12 are treatment plants.

On 8/18, the thresholds of 0.5 and 0.75 both had clusters composed solely of healthy or diseased plants. The 1.0 threshold had one cluster of healthy plants and one mixed cluster, composed of healthy and diseased plants. The results of the 0.5 and 0.75 thresholds were optimal with clear distinction of healthy plants from diseased plants, whereas the 1.0 threshold had one pure and one mixed cluster, which was not optimal. The results for 8/11 were similar to 8/18, with all three thresholds having one cluster of healthy plants and one cluster of diseased plants. These results were optimal for all three thresholds. On 8/4, results were still excellent for 0.5 and 0.75 thresholds with the 0.5 threshold having one cluster of healthy plants and three clusters of diseased plants, while the 0.75 threshold had one cluster of healthy plants and two clusters of diseased plants. The 1.0 threshold had one cluster of healthy plants and one mixed cluster. On 7/28, all three thresholds had one cluster of minimally (R1 and R2) diseased plants and one or more clusters of healthy and minimally (R1) diseased plants.

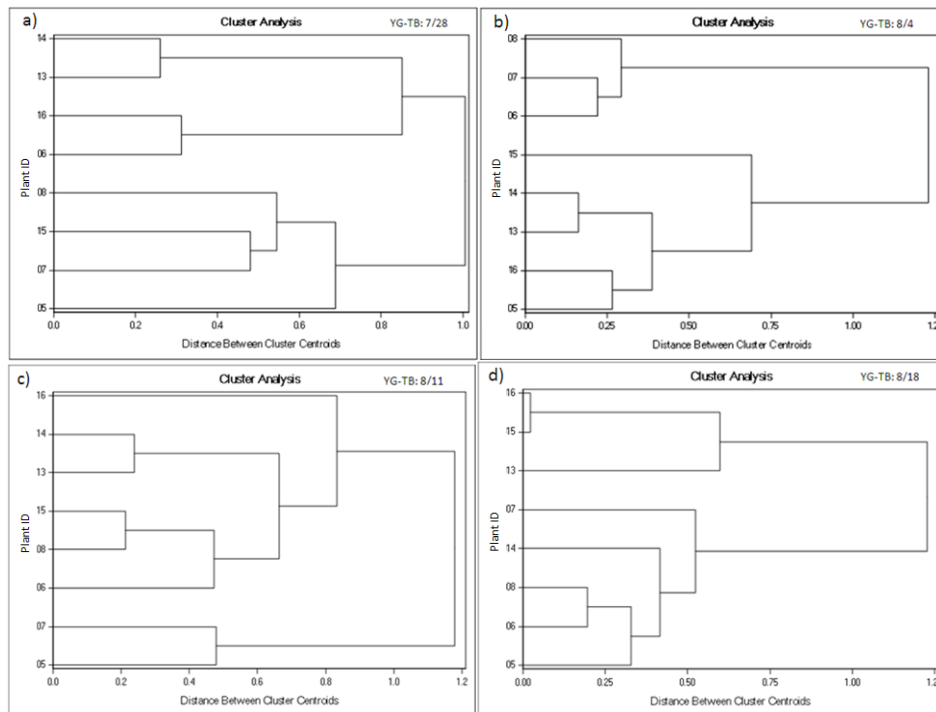


Figure 3. Tree diagrams for tuber bulking (TB) stage on: a) 7/28; b) 8/4; c) 8/11; d) 8/18. Plants 05, 06, 07, and 08 are control plants; plants 13, 14, 15, and 16 are treatment plants.

Table 2. YG – VG cluster membership for each disease rating by distance threshold.

		YG - VG Cluster Distribution											
		7/28			8/4			8/11			8/18		
		Membership %			Membership %			Membership %			Membership %		
Cluste	Rating	0.5	0.7	1.0	0.5	0.75	1.0	0.5	0.75	1.0	0.5	0.75	1.0
1	R0												33%
	R1	50	50	50%									
	R2	50	50	50%	100%	100	100						
	R4							75%	75%	75%			
	R5							25%	25%	25%	50%	50%	33%
	R6										50%	50%	33%
2	R0	75	67	67%			57%	100	100	100	100	100	100
	R1	25	33	33%									
	R2				100%	67%	29%						
	R4					33%	14%						
3	R0	50				100					100	100	
	R1	50											
	R2				50%								
	R4				50%								
4	R0				100%						100		

The 1.0 threshold did not differentiate pure clusters of healthy or diseased plants as well as the 0.5 and 0.75 thresholds. The 0.75 threshold was superior to the 0.5 threshold since it provided nearly the same solution, but with fewer mixed clusters and fewer clusters overall. Cluster analysis was capable of differentiating diseased (R2-R6) plants from healthy (R0) plants, but was incapable of differentiating minimally diseased (R1) plants from healthy (R0) plants on 7/28.

Table 3. YG – TB cluster membership for each disease rating by distance threshold.

YG - TB Cluster Distribution													
		7/28			8/4			8/11			8/18		
		Membership %			Membership %			Membership %			Membership %		
Cluste	Rating	0.5	0.75	1.0	0.5	0.75	1.0	0.5	0.75	1.0	0.5	0.75	1.0
1	R0			25%	100%	100%	100%			33%			
	R2	100	100	75									
	R5							100%	100	67%			
	R6										100%	100%	100%
2	R0	50%	50%	75		20%	20		40%	100		80%	80%
	R2	50%	50%										
	R3			25		20%	20						
	R4				100%	60%	60%						
	R5							100%	60%				
	R6										100%	20%	20%
3	R0	100	75%		25%			67%	100		100%		
	R3		25%		25%								
	R4				50%								
	R5							33%					
4	R0	50%						100%			75%		
	R3	50%											
	R6										25%		
5	R0	100											

Vegetative Indices

Analysis using vegetative indices was completed for the 10 measurement events using wavelengths determined to be most sensitive when comparing diseased plant reflectance indices to healthy plant reflectance indices. For brevity, four measurement events for each experiment using SR and NDVI indices for the VG and TB stages, respectively, are displayed in Table 4. Index wavelengths are listed by experiment.

For the VG stage, SR and NDVI ranged from 13.005 and 0.662 for healthy (R0) plants to 4.099 and 0.277 for diseased (R5 and R6) plants, while SR and NDVI for the TB stage ranged from 5.118 and 0.677 for healthy (R0) plants to 4.540 and 0.515 for diseased (R6) plants.

Table 4. SR and NDVI indices for vegetative (VG) and tuber bulking (TB) stages.

Date	7/28		8/4		8/11		8/18	
Group	Contr	Treatment	Contro	Treatment	Control	Treatment	Contro	Treatment
VG Stage								
Ratin	R0	R1, R2	R0	R2, R4	R0	R4, R5	R0	R5, R6
SR^[a]	13.005	12.24	11.093	8.689	9.886	6.167	8.826	4.099
NDVI^[c]	0.662	0.651	0.61	0.541	0.556	0.411	0.44	0.277
TB Stage								
Ratin	R0	R2, R3	R0	R3, R4	R0	R5, R6	R0	R6
SR^[a]	5.118	7.107	5.330	6.432	4.790	6.230	4.599	4.540
NDVI^[c]	0.677	0.741	0.687	0.710	0.672	0.668	0.665	0.515

^[a]SR = 770 nm / 665 nm; ^[b]NDVI = (945 nm – 695 nm) / (945 nm + 695 nm); ^[c]NDVI = (735 nm – 670 nm) / (735 nm + 670 nm)

Focusing on the VG stage, ANOVA results comparing healthy plant index means to diseased plant index means for 7/28 to 8/18 were $F_{(1,12)} = 5.75$, $p = 0.0336$ for SR and $F_{(1,12)} = 3.34$, $p = 0.0924$ for NDVI; for 8/4 to 8/18, the results were $F_{(1,8)} = 17.8$, $p = 0.0029$ for SR and $F_{(1,8)} = 7.52$, $p = 0.0253$ for NDVI; and finally for 8/11 to 8/18, the results were $F_{(1,4)} = 33.49$, $p = 0.0044$ for SR and $F_{(1,4)} = 10.29$, $p = 0.0326$ for NDVI. The results illustrated a significant difference between the mean index values for healthy plants and diseased plants, which increased in significance with the progression of the disease over the timeframes specified. To determine at what point the difference between indices of healthy plants and diseased plants became significant for the measurement events listed in Table 4, a two-sample t-test was completed using the indices for each healthy and diseased plant at each measurement event. The results for 7/28 were $t_{(6)} = 1.16$, $p = 0.292$ for SR and $t_{(6)} = 0.97$, $p = 0.368$ for NDVI; the results for 8/4 were $t_{(6)} = 4.09$, $p = 0.0064$ for SR and $t_{(6)} = 4.57$, $p = 0.0038$ for NDVI; the results for 8/11 were $t_{(6)} = 5.49$, $p = 0.0015$ for SR and $t_{(6)} = 5.74$, $p = 0.0012$ for NDVI; and finally the results for 8/18 were $t_{(6)} = 8.15$, $p = 0.0002$ for SR and $t_{(6)} = 4.33$, $p = 0.0049$ for NDVI. These results indicated that the indices for healthy (R0) plants and diseased (R1 and R2) plants were not significantly different on 7/28, but starting with 8/4, the indices for healthy and diseased plants were significantly different.

DISCUSSION

Early detection of disease infestation within crops is essential to reduce potential production losses, reduce the risk of ground water contamination from over-application of pesticides, and reduce the cost of farming. This experiment used several methods to determine the efficacy of spectral reflectance data to differentiate diseased plants from healthy plants. Cluster analysis of reflectance spectra demonstrated that diseased plants could be differentiated from healthy plants. The results for the VG stage of growth, with a centroid distance threshold of 0.75, illustrated that clustering analysis could differentiate diseased (R2-R6) plants from healthy (R0) plants but could not discern minimally diseased (R1) plants from healthy (R0) plants at early stages of disease progression. These results were similar to results found by [42] using cluster analysis to discriminate late blight infected tomato plants from healthy tomato plants. [42] was able to differentiate more heavily diseased plants from healthy plants, but was unable to differentiate minimally diseased plants from healthy plants. Analysis using the vegetative indices SR and NDVI demonstrated that diseased plants could be successfully differentiated from healthy plants. The results for the VG stage were similar to results found by [25] using SR and NDVI to discriminate late blight infected potato plants from healthy plants. In this experiment, the plants in the VG stage ranged from 13.005 to 4.009 and 0.662 to 0.277 for healthy to diseased (R5 and R6) for SR and NDVI, respectively, while [25] found values in the range of 10.81 to 2.14 and 0.83 to 0.34 for healthy to 90% diseased plants. The minor differences in index values between this experiment and [25] were likely due to [25] capturing data on one measurement event only, whereas the data used in this experiment was captured on 10 separate measurement events over a five-week period and the disease rating levels used in [25] were not the same as the disease rating levels used in this experiment (Table 1). Looking beyond these differences, one can see how the SR and NDVI values drop as the disease progresses in both [25] and this experiment. The VG stage indices illustrated that SR and NDVI were not capable of differentiating minimally diseased (R1 and R2) plants from healthy (R0) plants, but as the disease severity increased after 7/28, SR and NDVI were both capable of differentiating diseased (R2-R6) plants from healthy (R0) plants (Table 4). The SR and NDVI results were in agreement with the clustering analysis results, which demonstrated the capacity to differentiate diseased (R2-R6) plants from healthy (R0) plants.

The wavelengths found to be the most sensitive for the calculation of SR (665 nm and 770 nm) and NDVI (670, 695, 735, and 945 nm), listed in Table 4, were similar to the optimal wavelengths (543, 663, 761, and 1993 nm) found by [42] while completing spectral change analysis on tomatoes infected with late blight. Similar wavelengths (540, 610, 620, 700, 710, 720, 730, 750, 780, and 1040 nm) were also found by [25] to be optimal for the discrimination of late blight infected potato plants. The wavelengths used in the calculation of the SR and NDVI indices were within the red visible wavelength region that corresponds to an area of high energy absorption by chlorophyll, which is adversely affected when a plant is infected with a disease [12]. When a plant suffers from a stress factor like drought or pest/disease infestation, normal chlorophyll production diminishes, followed by a decrease in absorption and an increase in reflectance in the blue and red visible regions. Reflectance within the NIR region is also reduced when the plant responds to pathogen invasion because the reflective capacity of the mesophyll layer decreases.

Plants with the disease rating level of R2 (Table 1) have small spots on more than two leaves, but less than half of the canopy with no "bull's eyes." Clustering analysis and the indices SR and NDVI for YG in the VG stage differentiated early blight infected plants from healthy plants starting at the R2 disease rating level. The ability to discern healthy plants from minimally diseased (R1) plants would have been optimal, but while the physiological changes in minimally diseased plants may alter their reflectance characteristics, changes do not reach the point where a significant difference can be established.

Detection of plants infected with early blight at the R2 disease level is possible when crop scouting, but positive identification of the disease would be challenging at the R2 level since the foliar symptoms of early blight generally appear on older leaves lower on the canopy, which would be more difficult to locate [36]. According to [44], conventional ground scouting has not provided an efficient means of disease detection and monitoring of crops. Detection of early blight infected plants using clustering analysis or vegetative indices like SR or NDVI may provide a valuable resource for crop scouting since these methods provide detection of disease throughout the entire field, which would be challenging for crop scouting alone since disease infestation is predominately concentrated in patches around original foci where disease originates [22] with large areas of fields free from disease at any stage of infestation [7].

CONCLUSION

Hyperspectral reflectance spectra captured twice weekly for five weeks from Yukon Gold potatoes grown to the VG (3–6 weeks) and TB (8–12 weeks) growth stages were analyzed using clustering analysis and vegetative indices SR and NDVI. Clustering analysis of the reflectance spectra was found to be capable of distinguishing early blight diseased plants from healthy plants. At the optimal centroid distance threshold of 0.75, clustering analysis successfully segregated pure unmixed clusters composed of diseased (R2-R6) plants from healthy (R0) plants, but was unable to segregate minimally diseased (R1) plants from healthy (R0) plants. Analysis of reflectance spectra using vegetative indices SR and NDVI was effective at differentiating moderately diseased plants from healthy plants. The diseased plants could be differentiated from healthy plants starting at the R2 disease rating level on the second measurement event and for the remainder of the measurement events examined. The wavelengths found to be most sensitive for the calculation of the indices were 665 nm and 770 nm for SR and 670, 695, 735, and 945 nm for NDVI.

Both clustering analysis and vegetative indices proved to be useful options for the differentiation of diseased plants from healthy plants once the disease had progressed to the disease rating level of R2. The ability to discern healthy plants from minimally diseased (R1) plants would have been optimal, but while the physiological changes in minimally diseased plants may alter their reflectance characteristics, changes do not reach the point where a significant difference can be established.

The plants used for this experiment were grown in closed chambers and reflectance data was captured in a greenhouse environment. Additional research should be conducted to substantiate the results obtained in this experiment and to determine whether these results differ from field based results.

REFERENCES

- [1] Apan, A., Datt, B., & Kelly, R. 2005. Detection of Pests and Disease in Crops Using Hyperspectral Sensing: Comparison of Reflective Data for Different Symptoms. *Proceedings of SSC 2005 Spatial Intelligence and Innovation*, 10-18.
- [2] ASD, Inc. 2010. Field Spec 3 User Manual. Boulder, CO, USA.
- [3] ASD Inc. FS4. 2014, December 19. *ASD Inc. FieldSpec Product Listing*. Retrieved from ASD Inc.: <http://www.asdi.com/products/fieldspec-spectroradiometers>
- [4] Backoulou, G., Elliott, N., Giles, K., Phoofolo, M., & Catana, V. 2011. Development of a method using multispectral imagery and spatial pattern metrics to quantify stress to wheat fields caused by *Diuraphis noxia*. *Computers and Electronics in Agriculture*, 75, 64-70.
- [5] Blackburn, G. 1998a. Spectral indices for estimating photosynthetic pigment concentrations: a test using senescent tree leaves. *International Journal of Remote Sensing*, 4, 657-675.
- [6] Blackburn, G. 1998b. Quantifying Chlorophylls and Carotenoids at Leaf and Canopy Scales: An Evaluation of Some Hyperspectral Approaches. *Remote Sensing of the Environment*, 66, 273-285.
- [7] Bravo, C., Moshou, D., West, J., McCartney, A., & Ramon, H. 2003. Early Disease Detection in Wheat Fields using Spectral Reflectance. *Biosystems Engineering*, 2, 137-145.
- [8] Canadian Food Inspection Agency. 2013, December 20. *Yukon Gold*. Ontario: Canadian Food Inspection Agency. Retrieved from Canadian Food Inspection Agency: <http://www.inspection.gc.ca/plants/potatoes/potato-varieties/yukon-gold/eng/1312587385949/1312587385950>
- [9] Chen, P., Haboudane, D., Tremblay, N., Wang, J., Vigneault, P., & Li, B. 2010. New spectral indicator assessing the efficiency of crop nitrogen treatment in corn and wheat. *Remote Sensing of the Environment*, 114, 1987-1997.
- [10] Gitelson, A., Kaufman, Y., Stark, R., & Rundquist, D. 2002. Novel algorithms for remote estimation of vegetation fraction. *Remote Sensing of the Environment*, 80, 76-87.

- [11] Gitelson, A., Keydan, G., & Merzlyak, M. 2006. Three-band model for noninvasive estimation of chlorophyll, carotenoids, and anthocyanin contents in higher plant leaves. *Geophysical Research Letters*, 33, 1-5.
- [12] Gitelson, A., Merzlyak, M., & Chivkunova, O. 2001. Optical Properties and Nondestructive Estimation of Anthocyanin Content in Plant Leaves. *Photochemistry and Photobiology*, 1, 38-45.
- [13] Gitelson, A., Zur, Y., Chivkunova, O., & Merzlyak, M. 2002. Assessing Carotenoid Content in Plant Leaves with Reflectance. *Photochemistry and Photobiology*, 3, 272-281.
- [14] Govaerts, Y., Verstraete, M., Pinty, B., & Gobron, N. 1999. Designing optimal spectral indices: a feasibility and proof of concept study. *International Journal of Remote Sensing*, 9, 1853-1873.
- [15] Haboudane, D., Tremblay, N., Miller, J., & Vigneault, P. 2008. Remote Estimation of Crop Chlorophyll Content Using Spectral Indices Derived From Hyperspectral Data. *IEEE Transactions on Geoscience Remote Sensing*, 2, 423-437.
- [16] Hansen, P., & Schjoerring, J. 2003. Reflectance measurement of biomass and nitrogen in wheat crops using normalized difference vegetation indices and partial least squares regression. *Remote Sensing of Environment*, 86, 542-553.
- [17] Huang, W., Lamb, D., Niu, Z., Zhang, Y., Liu, L., & Wang, J. 2007. Identification of yellow rust in wheat using in-situ spectral reflectance measurements and airborne hyperspectral imaging. *Precision Agriculture*, 8, 187-197.
- [18] Jacquemoud, S., & Ustin, S. 2001. Leaf Optical Properties: A State of the Art. *8th International Symposium of Physical Measurements & Signatures in Remote Sensing, CNES*, 223-232.
- [19] Jain, N., Ray, S., Singh, J., & Panigrahy, S. 2007. Use of hyperspectral data to assess the effects of different nitrogen applications on a potato crop. *Precision Agriculture*, 225-239.
- [20] Jensen, J. R. 2005. *Introductory Digital Image Processing: a Remote Sensing Perspective*. Upper Saddle River: Pearson Prentice Hall.
- [21] Jones, H., & Vaughan, R. 2010. *Remote Sensing of Vegetation* (1st ed.). Oxford: Oxford University Press.
- [22] Moshou, D., Bravo, C., West, J., Wahlen, S., McCartney, A., & Ramon, H. 2004. Automatic detection of 'yellow rust' in wheat using reflectance measurements and neural networks. *Computers Electronics in Agriculture*, 44, 173-188.
- [23] Pavlista, A. 1995. *EC95-1249 Potato Production Stages: Scheduling Key Practices*. Lincoln: Historical Materials from University of Nebraska-Lincoln Extension.
- [24] Prabhakar, M., Prasad, Y. G., Thirupathi, M., Sreedevi, G., Dharajothi, B., & Venkateswarlu, B. 2011. Use of ground based remote sensing for detection of stress in cotton. *Computers and Electronics in Agriculture*, 79, 189-198.
- [25] Ray, S., Jain, N., Aroa, R., Chavan, S., & Panigrahy, S. 2011. Utility of Hyperspectral Data for Potato Late Blight Disease Detection. *Journal of Indian Society of Remote Sensing*, 2, 337-354.
- [26] Rodriguez-Perez, J., Riano, D., Carlisle, E., Ustin, S., & Smart, D. 2007. Evaluation of Hyperspectral Reflectance Indexes to Detect Grapevine Water Status in Vineyards. *American Journal for Enology and Viticulture*, 3, 302-317.
- [27] Rollin, E., & Milton, E. 1998. Processing of High Spectral Resolution Reflectance Data for the Retrieval of Canopy Water Content Information. *Remote sensing of the Environment*, 65, 86-92.
- [28] SAS Institute. 2014. *SAS User's Guide*. Version 9.3. Cary, NC, U.S.A.
- [29] SAS Institute Inc. 2008a. *SAS/STAT® 9.2 User's Guide [Clustering Procedures]*. Cary, NC: SAS Institute Inc.
- [30] SAS Institute Inc. 2008b. *SAS/STAT® 9.2 User's Guide [TREE Procedure]*. Cary, NC: SAS Institute Inc.
- [31] Schumann, G., & D'Arcy, C. 2010. *Essential Plant Pathology*. St. Paul: The American Phytopathological Society.
- [32] Serrano, L., Penuelas, J., & Ustin, S. 2002. Remote sensing of nitrogen and lignin in Mediterranean vegetation from AVIRIS data: Decomposing biochemical from structural signals. *Remote Sensing of the Environment*, 81, 355-364.
- [33] Shafri, H., & Hamden, N. 2009. Hyperspectral Imagery for Mapping Disease Infection in Oil Palm Plantation Using Vegetation Indices and Red Edge Technique. *American Journal of Applied Sciences*, 6, 1031-1035.
- [34] Tarpley, L., Reddy, K., & Sassenrath-Cole, G. 2000. Reflectance Indices with Precision and Accuracy in Predicting Cotton leaf Nitrogen Concentration. *Crop Science*, 40, 1814-1819.
- [35] Thenkabail, P., Smith, R., & De Pauw, E. 2002. Evaluation of Narrowband and Broadband Vegetation Indices for Determining Optimal Hyperspectral Wavebands for Agricultural Crop Characterization. *Photogrammetric Engineering & Remote Sensing*, 6, 607-621.
- [36] Wharton, P., & Kirk, W. 2007. *Early Blight - Extension Bulletin E-2991*. East Lansing: Michigan State University.
- [37] Xue, L., Cao, W., Luo, W., Dai, T., & Zhu, Y. 2004. Monitoring Leaf Nitrogen Status in Rice with Canopy Spectral Reflectance. *Agronomy Journal*, 96, 135-142.

- [38] Yang, C., Everitt, J., & Bradford, J. 2006. Comparison of QuickBird Satellite Imagery and Airborne Imagery for Mapping Grain Sorghum Yield Patterns. *Precision Agriculture*, 7, 33-44.
- [39] Yang, F., Li, J., Gan, X., Qian, Y., Wu, X., & Yang, Q. 2010. Assessing nutritional status of *Festuca arundinacea* by monitoring photosynthetic pigments from hyperspectral data. *Computers and Electronics in Agriculture*, 70, 52-59.
- [40] Yao, H., Huang, Y., Hruska, Z., Thomson, S., & Reddy, K. 2012. Using Vegetation Index and Modified Derivative for Early Detection of Soybean Injury from Glyphosate. *Computers and Electronics in Agriculture*, 145-157.
- [41] Yi, Q., Bao, A., Wang, Q., & Zhao, J. 2013. Estimation of leaf water content in cotton by means of hyperspectral indices. *Computers and Electronics in Agriculture*, 90, 144-151.
- [42] Zhang, M., Liu, X., & O'Neill, M. 2002. Spectral discrimination of *Phytophthora infestans* infection on tomatoes based on principal component and cluster analyses. *International Journal of Remote Sensing*, 23, 1095-1107.
- [43] Zhang, M., Qin, Z., & Liu, X. 2005. Remote Sensed Spectral Imagery to Detect Late Blight in Field Tomatoes. *Precision Agriculture* 6, 489-508.
- [44] Zhang, M., Qin, Z., Liu, X., & Ustin, S. 2003. Detection of stress in tomatoes by late blight disease in California, USA, using remote sensing. *International Journal of Applied Earth Observation and Geoinformation*, 295-310.
- [45] Zhao, D., Reddy, K., Kakani, V., & Reddy, V. 2005. Nitrogen deficiency effects on plant growth, leaf photosynthesis, and hyperspectral reflectance properties of sorghum. *European Journal of Agronomy*, 22, 391-403.

International Journal of Plant, Animal and Environmental Sciences

